

DESY SR-72/11
July 1972

Optical and Photoelectric Properties of the
Lead Chalcogenides

by

M. Cardona and C. M. Penchina
Max-Planck-Institut für Festkörperforschung, Stuttgart

E. E. Koch, P. Y. Yu
Deutsches Elektronen-Synchrotron DESY, Hamburg

To be sure that your preprints
are promptly included in the
HIGH ENERGY PHYSICS INDEX, send
them to the following address
(if possible by air mail):

DESY
Bibliothek
2 Hamburg 52
Notkestieg 1
Germany

Optical and Photoelectric Properties of the
Lead Chalcogenides

Manuel Cardona and Claude M. Penchina⁺

Max-Planck-Institut für Festkörperforschung,
Stuttgart, German Federal Republic

and

E.E. Koch^x, P.Y. Yu^{*}

Deutsches Elektronen-Synchrotron,
Hamburg, German Federal Republic

A B S T R A C T

The reflection spectra of PbS, PbSe and PbTe have been measured in the 14-26eV region using as a source the DESY-synchrotron. Three peaks are observed for PbSe and PbTe and two for PbS, corresponding to transitions from the outermost d-levels of the Pb core to the conduction bands. In order to find out the relationship between these peaks and the spin-orbit splitting of the d core levels, X-rays photoemission measurements (ESCA) have been performed. It is concluded that this spin-orbit splitting of the d core levels does not appear directly in the optical spectra. A simple model is given to interpret these spectra.

^x Permanent address: Sektion Physik der Universität München.

^{*} Present address : Physics Department, University of
California-Berkeley.

⁺ Permanent address: Dept. of Physics & Astronomy, University of
Massachusetts, Amherst, Massachusetts, 01002
supported in part by the National Science
Foundation.

The valence band, and other core levels of binding energies in the range of the K α line (1486.6 eV) Aluminium-X-ray source have also been studied. The binding energies, splittings, and chemical shifts obtained are discussed and compared with theoretical calculations. The most intense ESCA lines exhibit satellites which can be associated with lines produced by the excitation of valence plasmons. The effects of adsorbed oxygen on the ESCA spectra are also discussed.

INTRODUCTION

The lead chalcogenides (PbS, PbSe, and PbTe) crystallize in the rock salt structure. Because of the simplicity of this structure and of the considerable technological interest of these materials,¹ their electronic properties have been the object of a large number of experimental and theoretical studies.²⁻⁴ Their intrinsic optical properties from 1 to 22 eV were measured by Cardona and Greenaway⁵ and the photoemission by Spicer and Lapeyre.⁶ An assignment of the observed optical structure in terms of transitions between valence and conduction bands at critical points was made by Lin and Kleinman.⁷ Beside the transitions originating at the valence bands, some indication of core transitions (originating at the outermost d-levels of the Pb core) was seen in Ref. 5 between 18 and 22 eV. However, the discrete gas discharge source used in these measurements did not allow a detailed study of this core structure. Characteristic electron energy loss measurements (CEL) have indicated the existence of more than one peak due to transitions from these core d electrons.⁸

The inadequacies of conventional vacuum uv spectroscopic sources are fully overcome by the use of synchrotron radiation.⁹ Transmission measurements on PbS, PbSe, PbTe, using as a source the radiation of the DESY electron synchrotron in the region from 36-150 eV, have recently appeared.¹⁰ Unfortunately, in this region only broad Fano-Cooper maxima,¹¹ associated with the delayed transitions from the d core states to the conduction band continua, are observed. These absorption measurements were not extended to lower energies because of absorption in the carbon substrates onto which the films were deposited. It was not possible to prepare unsupported thin films of these easily cleaved materials.

In this work we present the reflection spectra of PbS, PbSe, and PbTe in the region from 14 to 26 eV, as obtained with synchrotron radiation. In this energy region, structure related to the d-electrons of the lead core is seen: three peaks in PbSe and PbTe and two in PbS. In similar recent work on the III-V compounds¹² it was possible to extract from the d-electron structure doublets associated with the spin-orbit splitting of the core d levels. In view of large discrepancies in the available theoretical calculations of the spin-orbit splittings of the Pb 5d (O_{IV-V}) levels of the lead chalcogenides^{4,13} we have measured the x-ray photoemission spectra (ESCA) of these materials. The spin-orbit splitting of the 5d electrons of Pb obtained with this technique permits us to conclude that no doublet directly related to this splitting appears in the reflection spectra. This fact, in contrast to the situation for the III-V compounds, is related to the strong spin-orbit effects present in the conduction bands of the lead chalcogenides (6p electrons of Pb). Under these conditions, a quantitative interpretation of the optical spectra from 14 to 26 eV requires a detailed computer calculation of the optical constants, using

the band structure with spin-orbit interactions and the correct optical matrix elements. Such calculation has yet to be performed. In its stead, we propose a simple qualitative model to interpret the observed structure on the basis of $5d+6p$ excitations within the Pb ions and the spin-orbit and crystal field splittings of these levels.

The ESCA measurements, performed with the Al $K\alpha$ radiation, yield also information about other core levels with binding energies lower than 1486.6 eV and about the density of states of the valence bands. The core energies so obtained are discussed in terms of the chemical shifts with respect to the pure elements. Comparison is also made with band structure calculations of the energy of these core levels. The observed peaks in the density of valence states agree with estimates from existing band structure calculations.

The stronger ESCA lines of both constituents exhibit satellites which can be related to the creation of valence electron plasmons. Additional shifted Pb and Te lines, due to the absorption of oxygen at the sample surface, have also been observed. These lines disappear after bombardment with argon ions.

MEASUREMENTS

The details of the optical and ESCA experiments have been discussed elsewhere.¹²

The samples for reflection measurements were epitaxial layers, vacuum deposited on KCl and also a natural single crystal of PbS.

The ESCA measurements were performed on polycrystalline samples prepared by vacuum deposition on a metal substrate heated to 200°C. A cleaved p-type natural crystal of PbS was also

measured, with results essentially identical to those obtained with the evaporated sample. The PbS and PbTe samples were found to have p-type thermoelectric power while the PbSe sample showed the opposite behaviour. The 283.8 eV line of carbon¹⁴ was used as a reference. Measurements were always performed before and after bombarding the sample with argon ions.

RESULTS

a) Optical Measurements.

Figure 1 shows the reflectivity spectra of PbS (natural crystal), PbSe, and PbTe (epitaxial films) at room temperature for photon energies between 14 and 26 eV, in arbitrary units. The solid arrows indicate the position of the peaks observed in the CEL spectrum by Lahaye et al.⁸ The dashed arrows represent the CEL peaks observed by Leder.¹⁵ The optical measurements show more structure than either of the CEL measurements which were made with relatively low resolution (1 eV in Ref. 8, > 1 eV in Ref. 15). The agreement between the optical and the CEL measurements and also that of the CEL measurements of Refs. 8 and 15 with each other, is not totally satisfactory. However, one must point out that reflectivity peaks are often shifted by as much as a line width with respect to peaks in $\text{Im}(1/\epsilon)$ measured with CEL. Because of the small energy range available, no direct comparison was made through a Kramers-Kronig analysis of the data. The energies of the peaks in Figure 1, and of the CEL peaks of Refs. 8 and 15, are given in Table I.

b) ESCA Measurements

The x-rays photoemission spectra of the 5d levels of Pb, and those of the 3d levels of Se and the 4d levels of Te in

argon-ion bombarded PbS, PbSe, and PbTe are shown in Fig. 2. It is clear in view of these results that, the spin-orbit splitting of the 5d levels of Pb (2.6 eV) does not correspond systematically to any of the splittings of Fig. 1. (The fact that the A-C splitting in PbSe is 2.6 eV should be regarded as fortuitous). The binding energies of these and the other ESCA peaks observed with the $K\alpha$ line of Al are listed in Table II, together with the corresponding levels of the pure elements.¹⁶ The measurements are, as usual, referred to the Fermi level of the semiconductor.¹⁸ Except for uncertainties in the position of the Fermi level with respect to the band edges, the accuracy of the binding energies in Table II should be that of the calibration line of carbon (0.3 eV)¹⁴ since our retarding voltage measurements were accurate to better than 0.05 eV. For the standard carrier densities present in these materials the Fermi level of the bulk should be within 0.1 eV from the appropriate band edge (valence for the p-type PbS and PbTe, conduction for the n-type PbSe). Some existing work seems to indicate that no surface pinning of the Fermi energy occurs for clean surfaces of these materials.¹⁹ We note that we have resolved the $L_{III}-L_{II}$ spin-orbit splitting of S, the M_V-M_{IV} of Se, and the N_V-N_{IV} of Te. These splittings appear unresolved in Ref. 16. The observed splittings agree reasonably well with the atomic calculations of Ref. 17 (1.34 eV for $L_{III}-L_{II}$ in S, 0.98 eV for M_V-M_{IV} in Se, 1.59 eV for N_V-N_{IV} in Te.)

The chemical shifts between the pure element and the compound are, within the experimental error, the same for all levels of a given atom in a given compound, with the possible exception of those which give weak and uncertain ESCA peaks

(all s-levels, O_{III} and N_{II} of Pb, N_{III} , N_{II} of Te). The averages of these chemical shifts (excluding the anomalously inaccurate ones just mentioned) are given in Table III.

Figure 3 shows the x-ray photoemission spectra of PbS, PbSe, and PbTe near the zero binding energy threshold. The data extend to nominally negative binding energies, as a result of the finite resolution of the system. These measurements were taken with an electron analyzer voltage of 50 V (those in Fig. 2 with 20 V). Consequently the total spectral width of Fig. 3, including source width and analyzer resolution, is somewhat poorer than in Fig. 2. Spectral resolution is composed of two terms, an instrumental linewidth proportional to analyzer voltage and the natural width of the exciting x-ray line. From the failure to resolve the M_V - M_{IV} splitting of Se with a 50V analyzer, we estimate the spectral width of Fig. 3 at ± 1 eV; this is just the width required to explain the negative energy tail of Fig. 3.

The adsorption of oxygen at the surface of the materials under consideration has received considerable attention.¹⁹⁻²¹ The presence of oxygen at the surface of our samples can be easily detected in the ESCA spectra. All ESCA lines appear split (PbTe) or broadened asymmetrically towards higher binding energies (PbS, PbSe) after exposure to air. Beside the lines characteristic of the lead chalcogenide, satellites with higher binding energies appear. These satellites disappear after bombarding with argon ions. At the same time, the always present K line of oxygen (532.0 eV) decreases in strength. Typical examples of the splitting of ESCA lines in PbTe due to oxygen contamination are shown in Fig. 4. The average shift of the oxide lines of Pb with respect to those of PbTe is

1.95 eV. We list these lines in Table II under the label "PbO". In spite of the unknown structure of this oxide, the "PbO" lines fit well into the PbTe→PbSe→PbS→PbO systematics of Table II. The corresponding average shift observed for the oxide lines of Te is 4.0 eV.

It has been reported¹⁹ that the Fermi energy is not pinned at a clean surface of a lead chalcogenide. However, oxygen adsorption introduces surface states and makes the surfaces strongly n-type. As a result, the lines of PbTe, PbSe, and PbS exposed to air shift to slightly higher binding energies after cleaning by argon bombardment. The average shift observed is 0.15 eV for PbS and PbTe and 0.4 eV for PbSe.

The presence of plasmon satellites is a common occurrence in the ESCA spectra of metals.¹⁸ We have observed plasmon satellites associated with a number of strong ESCA lines of the lead chalcogenides. As shown in Fig. 5 these lines correspond to nominally larger binding energies. They are shifted from the parent line by the energy of the bulk plasmon (note some residual Te-O lines in the Te $M_{V,IV}$ spectra of Fig. 5). The plasmon energies determined from these shifts are listed in Table IV together with the plasmon energies determined by the CEL method.^{8,15}

DISCUSSION

As already mentioned, the original purpose of this combined synchrotron radiation and ESCA work was the interpretation of the spectra of Fig. 1. Figure 2 and Table II shows no obvious replica of the spin-orbit splitting of the $O_{IV,V}$ levels of Pb. Such replicas are standard in the corresponding spectra of zincblende-type semiconductors.¹² In order to explain the dif-

ference between these two classes of materials we look for differences in the structure of the final states for the transitions of Fig. 1, i.e., the conduction bands.

The lowest conduction bands of a zincblende-type material, e.g., InAs are hybridized 4s and 4p states of the In with a weak admixture of 3s and 3p states of As. These states have very small spin-orbit splittings (0.4 eV) and within the resolution of observed optical structure we need only treat orbital bands (i.e., we can neglect the spin). Under these conditions we would expect to find for the absorption originating at the d core levels (e.g., $N_{V,IV}$ of In) two similar bands, originating at N_V and N_{IV} respectively, and with relative weights 3 and 2 corresponding to the degeneracy of the N_V and N_{IV} states. This type of spectrum has indeed been observed in the III-V compounds.¹²

The lowest conduction bands of the lead chalcogenides, however, are formed of 6p wave functions of lead, with a large spin-orbit splitting ($\Gamma_6^- - \Gamma_8^-$ splitting $\cong \Delta \approx 2$ eV, see Fig. 6). **In order to calculate** the optical spectra of transitions from the core states it is therefore not sufficient to know the density of conduction states but we must have the spin composition of the conduction bands. The absorption peaks for transitions from the lead O_V and O_{IV} levels can thus occur at different energies.

A calculation of the optical constants including matrix elements for the spin eigenfunctions of the lead chalcogenides has yet to be performed. However, it is possible to give a qualitative model which explains the behaviour of Fig. 1. The initial states O_V and O_{IV} have total angular momentum $j = \frac{5}{2}$ and $j = \frac{3}{2}$, respectively. The final states are p-like and have,

in the absence of crystal field, $j = \frac{3}{2}$ (Γ_8^-) and $j = \frac{1}{2}$ (Γ_6^-). Allowed transitions require a change in total j equal to 0 or ± 1 . Hence only the following transitions are allowed

$$\begin{aligned} O_V (j = \frac{5}{2}) &\rightarrow \Gamma_8^- (j = \frac{3}{2}) \\ O_{IV} (j = \frac{3}{2}) &\rightarrow \Gamma_6^- (j = \frac{1}{2}) \\ \left[O_{IV} (j = \frac{3}{2}) &\rightarrow \Gamma_8^- (j = \frac{3}{2}) \right] \end{aligned} \quad (1)$$

A simple calculation using for O_{IV} , O_V pure d and for Γ_6^- , Γ_8^- pure p wave functions yields for the $O_{IV} (j = \frac{3}{2}) \rightarrow \Gamma_8^- (j = \frac{3}{2})$ transitions oscillator strengths 10 times smaller than those for the other two transitions of Eq. 1. (See Appendix A) We therefore neglect these transitions, as symbolized by the brackets in Eq. 1. Because of the large $\Gamma_8^- - \Gamma_6^-$ splitting it is clear from Eq. (1) that no replica of the $O_{IV} - O_V$ splitting should appear in the optical spectra once the $O_{IV} \rightarrow \Gamma_8^-$ transitions are neglected. The crystal field should split the Γ_8^- state but not Γ_6^- . Thus it is possible to explain the triplets of Fig. 1 in the manner sketched in Fig. 7. The crystal field splitting, D , and any shift of the Γ_8^- conduction state have to be understood as either the average over the Brillouin zone or that in the region of maximum contribution to the density of states. The energies D and γ needed to fit with this model the spectra of Fig. 1 are listed in Table I.

The chemical shifts of Table III are all negative, in contrast to the shifts measured in zincblende-type semiconductors which are negative for the anion and positive for the cation.^{12,22} We show in Table V a comparison of the binding energies of the measured outermost core d levels with those obtained from band structure calculations.^{4,13} (Agreement is better with calculations of Ref. 13 than with those of Ref. 4). Because of possible un-

certainties in the Fermi energies at the surface we have measured the calculated binding energies from the center of the gap: these uncertainties should not be very important for these small band gap materials, (E_g is 0.32 eV for PbTe, 0.28 eV for PbSe, and 0.41 eV for PbS at room temperature). The calculated anion energies are higher than observed while those of lead are consistently lower, a fact which is easy to attribute in part to the neutral (not ionic) potentials used in the calculations. A negative (positive) charge in the anion (cation) would decrease (increase) the calculated binding energies, as required by the experimental results. Evidence for an ionic charge positive on the Pb atom has been obtained in recent calculations.²³

Qualitatively, one might expect $\delta = \delta_{\text{Pb}} - \delta_{\text{anion}}$ (from Table III) to be simply related to the ionicity of the compound, but the Pauling ionicity of the lead chalcogenides is nearly negligible.²⁴ The effective charges derived from infrared data are large but practically the same for all three compounds.²⁵

We also notice in Table III a rapid decrease of the anion shifts with increasing atomic number. Similar results, including a nearly vanishing chemical shift for Te and Sb, have also been reported for the III-V and the II-VI compounds.^{12,22} It is also interesting to note that the observed spin-orbit splitting of the $\text{Pb}(O_V - O_{IV})$ levels is considerably larger than that calculated in Ref. 4. However, it agrees quite well with the calculations of Ref. 13.

We would like to thank W. Gudat, M. Skibowski and B. Sonntag for valuable help with the optical experiments and for discussions. The assistance of G. Krutina with the ESCA measurements is also gratefully acknowledged.

	PbS	Pbse	PbTe
A	19.9	20.2	19.7
B	22.1	21.9	21.7
C	not resolved 22.5	22.8	22.9
CEL ^a		20.5 22.8	20.7 22.7
CEL ^b	≈ 21.8	22.0	21.7
D=C-A	≈ 2.6	2.6	3.2
γ	≈ 0.4	0.9	0.6
Δ ^(c)	2.1	2.2	2.3

TABLE I Energies (in eV) of the peaks A, B, and C observed in Fig. 1. Also, peaks observed in the characteristic energy loss spectrum (CEL) in the same region and parameters of the model of Fig. 7. The $O_{IV,V}$ spin orbit splitting is 2.6 eV, as obtained from the ESCA measurements.

- a) From Ref. 8
- b) From Ref. 15
- c) From Ref. 13

Pb^(a) "PbO" PbS PbSe PbTe

O _V	19.2	18.6	18.25	18.15	17.80
O _{IV}	21.8	21.3	20.85	20.75	20.4
O _{III}	86.0		83	83.5	82.3
O _{II}	104.8		106.6	106.2	
O _I	147.3				
N _{VII}	138.1	137.5	137.1	136.95	136.5
N _{VI}	142.9	142.4	141.95	141.8	141.35
N _V	412.9		412.15	412.15	411.8
N _{IV}	435.2		434.35	434.35	433.95
N _{III}	644.5		643.55	643.7	643.35
N _{II}	763.9			762	761.5
N _I	893.5		891.5	892.3	891.7

TABLE II

Binding energies (in eV) of core levels found with x-ray photoelectron spectroscopy for the lead chalcogenides, as compared with the values reported for the pure elements in Ref. 16. The Pb lines labeled PbO are those obtained from the "oxide" spectrum of PbTe.

	S ^(a)	PbS		Se ^(a)	PbSe		Te ^(a)	PbTe
L _{III}		160.25	M _V		52.65	N _V		38.9
	164.8			56.7			39.8	
L _{II}		161.5	M _{IV}		53.5	N _{IV}		40.25
L _I	229.2	222.4	M _{III}	161.9	159.1	N _{III}		
			M _{II}	168.2	164.65	N _{II}	110.2	
			M _I	231.5	227.92	N _I	168.3	167.25
			L _{III}	1435.8	1431.7	M _V	572.1	571.25
						M _{IV}	582.5	581.65
						M _{III}	818.7	818.0
						M _{II}	869.7	868.95

(a) From Ref.16

	PbS	PbSe	PbTe
δ_{Pb}	-0.9	-1.0	-1.45
δ_{anion}	-4.7	-2.4	-0.85
$\delta_{\text{Pb}} - \delta_{\text{anion}}$	3.8	1.4	-0.6

TABLE III Average chemical shifts of Pb(δ_{IV}) and S, Se, Te(δ_{VI}) in the lead chalcogenides. Also, $\delta = \delta_{\text{Pb}} - \delta_{\text{anion}}$. The shifts are given with respect to the binding energies of the elements as reported in Ref. 16.

	PbS	PbSe	PbTe
Pb($O_{\text{V,IV}}$)	15.3±0.3	15.0±0.4	
Pb(N_{VII})			14.6±0.2
Pb(N_{VI})			14.6±0.2
Pb(N_{IV})	15.6±0.4	15.2±0.4	
Te(M_{IV})			14.6±0.2
CEL ^(a)		15.8	15.0
CEL ^(b)	14.5	15.1	14.4
Reflectivity ^(c)	15	12.5	12

- (a) From Ref. 8
- (b) From Ref. 15
- (c) From Ref. 6

TABLE IV Energy of the valence plasmons as obtained with ESCA and other techniques.

	PbS	PbSe	PbTe
Pb(O_V)	18.25 (a) 13.1 (b) 17.8 (c)	18.15 (a) 13.4 (b) 15.9 (c)	17.8 (a) 13.0 (b) 13.85 (c)
Pb(O_{IV})	20.85 (a) 15.6 (b) 20.4 (c)	20.75 (a) 15.5 (b) 18.5 (c)	20.4 (a) 15.0 (b) 16.6 (c)
Se(M_V)		52.65 (a) 54.8 (c)	
Se(M_{IV})		53.5 (a) 55.75 (c)	
Te(N_V)			38.9 (a) 39.7 (c)
Te(N_{IV})			40.25 (a) 41.3 (c)

(a) This work

(b) Calculated, Ref. 4

(c) Calculated, Ref. 13

TABLE V Observed spin-orbit splittings of the outermost d levels of the cores of the lead chalcogenides, compared with the results of band structure calculations.

REFERENCES

1. See, for instance, Yu. I. Ravich, B.A. Efimova, and I.A. Smirnov, "Semiconducting Lead Chalcogenides", (Plenum Press, N.Y., 1970).
2. See, for instance, "Les Composés Semi-Conducteur IV-VI" (éditions du centre national de la recherche scientifique, Paris, 1968), also published in J. Physique Suppl. C4 to Vol. 29, 1968.
3. D.E. Aspnes and M. Cardona, Phys. Rev. 173, 714 (1968) and references therein.
4. H. Overhof, Phys. Stat. Sol. 37, 691 (1970).
5. M. Cardona and D.L. Greenaway, Phys. Rev. 133, A 1685 (1964).
6. W.E. Spicer and G.J. Lapeyre, Phys. Rev. 139, A565 (1965).
7. P.L. Lin and D. Kleinman, Phys. Rev. 142, 478 (1966).
8. B. Lahaye, F. Pradal, and C. Gout, Ref. 2, p. 137.
9. R.P. Godwin, Springer Tracts in Modern Physics, 51, 15 (1969).
10. M. Cardona and R. Haensel, Phys. Rev. B1, 2605 (1970).
11. U. Fano and J.W. Cooper, Rev. Mod. Phys. 40, 441 (1968).
12. W. Gudat, E.E. Koch, P.Y. Yu, M. Cardona, and C. Penchina, Phys. Stat. Sol., to be published.
13. F. Herman, R.L. Kortum, I.B. Ortenburger, and J.P. Van Dyke, Ref. 2, p.62.
14. S. Hagström and S.E. Karlsson, Arkiv Fysik 26, 451 (1964).
15. L.B. Leder, Phys. Rev. 103, 1721 (1956).
16. J.A. Bearden and A.F. Burr, Rev. Mod. Phys. 39, 125 (1967).
17. F. Herman and S. Skillman, Atomic Energy Levels (Prentice Hall Inc., Englewood Cliffs, N.J., 1963).
18. K. Siegbahn, C. Nordling, A. Fahlman, R. Nordberg, K. Hamrin, J. Hedman, G. Johannson, J. Bergmark, S.E. Karlsson, J. Lindgren, and B.L. Lindberg, ESCA (Almqvist and Wiksells, Uppsala, 1967).
19. M. Brodski and J.N. Zemel, Phys. Rev. 155, 780 (1967).
20. L.J. Hillebrand, J. Chem. Phys. 41, 3971 (1964).
21. M.J. Lee and M. Green, J. Phys. Chem. Solids, 27, 797 (1966).

22. C.J. Vesely and D.W. Langer, Phys. Rev. 4, 451 (1971).
23. Y.W. Tsang and M.L. Cohen, Solid State Commun. 10, 871 (1972).
24. L. Pauling, The Nature of the Chemical Bond, (Cornell Univ. Press, Ithaca, N.Y. 1960).
25. E. Burstein, S. Perkowitz, and M.H. Brodsky, Ref. 2. p. 79.
26. V. Heine, Group Theory in Quantum Mechanics, (Pergamon Press, London, 1960) p. 433.

FIGURE CAPTIONS

1. Reflection spectra of PbS, PbSe, and PbTe observed with synchrotron radiation at room temperature. The solid and broken arrows indicate the peaks reported in the CEL spectra of Refs. 8 and 15, respectively.
2. X-rays photoemission spectra (ESCA) of the outermost core d levels of PbS, PbSe and PbTe taken with the $K\alpha$ line of Al.
3. ESCA spectra of the valence bands of PbS, PbSe and PbTe taken at room temperature with the $K\alpha$ line of Al. The signal level in this Figure is an order of magnitude weaker than that of Fig. 2. The arrows indicate the peaks in the density of valence states expected on the basis of the calculations of Ref. 13. The dashed curves indicate raw data before correction for the $Al(K\alpha_{3,4})$ - produced precursor of the O_V level of Pb. Because of uncertainties, in this correction, the data stop at 8.5 eV.
4. ESCA lines due to the outermost core d electrons of Pb and Te in oxygen contaminated PbTe. The high energy components (Pb-O, Te-O) disappear after bombardment with argon ions. The vertical scale is that of Fig. 2 expanded by a factor of 2.
5. Some ESCA lines of PbTe showing the plasmon replicas and residual Te-O lines. The vertical scale is the same as that of Fig. 2. The plasmon replicas have been enlarged by a factor of 10.
6. Band structure of PbTe calculated by Herman et al. (Ref. 13).
7. Model proposed to explain the Triplet structure of Fig. 1. The energies A, B, C, Δ , D, and γ are given in Table I.

APPENDIX A

We want to calculate the relative intensities of all transitions from the $O_V(j = \frac{5}{2})$ and $O_{IV}(j = \frac{3}{2})$ states to the $j = \frac{3}{2}$ and $j = \frac{1}{2}$ conduction states (Fig. 7). If we assume that only one set of orbital states ($\ell = 2$) form the $j = \frac{5}{2}$ core states and only one set of $\ell = 1$ states form the final conduction states, the various oscillator strengths are determined by only one parameter.

We write the core states as:²⁶

$$\begin{aligned}
 (j = \frac{5}{2}, m_j = \frac{5}{2}) &= (m_\ell = 2, m_s = +) \\
 (\frac{5}{2}, \frac{3}{2}) &= \sqrt{\frac{1}{5}} (2, +) + \sqrt{\frac{4}{5}} (1, +) \\
 (\frac{5}{2}, \frac{1}{2}) &= \sqrt{\frac{2}{5}} (1, +) + \sqrt{\frac{3}{5}} (0, +) \\
 (\frac{5}{2}, -\frac{1}{2}) &= \sqrt{\frac{3}{5}} (0, +) + \sqrt{\frac{2}{5}} (-1, +) \\
 (\frac{5}{2}, -\frac{3}{2}) &= \sqrt{\frac{4}{5}} (-1, +) + \sqrt{\frac{1}{5}} (-2, +) \\
 (\frac{5}{2}, -\frac{5}{2}) &= (-2, +) \\
 (j = \frac{3}{2}, m_j = \frac{3}{2}) &= \sqrt{\frac{4}{5}} (2, +) - \sqrt{\frac{1}{5}} (1, +) \\
 (\frac{3}{2}, \frac{1}{2}) &= \sqrt{\frac{3}{5}} (1, +) - \sqrt{\frac{2}{5}} (0, +) \\
 (\frac{3}{2}, -\frac{1}{2}) &= \sqrt{\frac{3}{5}} (-1, +) - \sqrt{\frac{2}{5}} (0, +) \\
 (\frac{3}{2}, -\frac{3}{2}) &= \sqrt{\frac{4}{5}} (-2, +) - \sqrt{\frac{1}{5}} (-1, +)
 \end{aligned}$$

The wave functions of the final states are:

$$\begin{aligned}
 (\frac{3}{2}, \frac{3}{2}) &= (1, +) & (\frac{3}{2}, -\frac{3}{2}) &= (-1, +) \\
 (\frac{3}{2}, \frac{1}{2}) &= \sqrt{\frac{1}{3}} (1, +) + \sqrt{\frac{2}{3}} (0, +) & (\frac{3}{2}, -\frac{1}{2}) &= \sqrt{\frac{1}{3}} (-1, +) + \sqrt{\frac{2}{3}} (0, +) \\
 (\frac{1}{2}, \frac{1}{2}) &= \sqrt{\frac{2}{3}} (1, +) - \sqrt{\frac{1}{3}} (0, +) & (\frac{1}{2}, -\frac{1}{2}) &= \sqrt{\frac{2}{3}} (-1, +) - \sqrt{\frac{1}{3}} (0, +)
 \end{aligned}$$

The transition probabilities are obtained by calculating the matrix elements of:

$$p^+ = -\sqrt{\frac{1}{2}} (p_x + ip_y), \quad p^- = \sqrt{\frac{1}{2}} (p_x - ip_y), \quad p_z$$

between initial and final states. The only orbital matrix elements

of p^+ , p^- , and p_z which do not vanish are obtained from the table of coupling coefficients in Ref. 26

$$\begin{aligned}
 \langle 2,2 | p^+ | 1,1 \rangle &= P \\
 \langle 2,1 | p^+ | 1,0 \rangle &= \sqrt{\frac{1}{2}} P \\
 \langle 2,0 | p^+ | 1,-1 \rangle &= \sqrt{\frac{1}{6}} P \\
 \langle 2,1 | p_z | 1,1 \rangle &= \sqrt{\frac{1}{2}} P \\
 \langle 2,0 | p_z | 1,0 \rangle &= \sqrt{\frac{2}{3}} P \\
 \langle 2,-1 | p_z | 1,-1 \rangle &= \sqrt{\frac{1}{2}} P \\
 \langle 2,0 | p^- | 1,1 \rangle &= \sqrt{\frac{1}{6}} P \\
 \langle 2,-1 | p^- | 1,0 \rangle &= \sqrt{\frac{1}{2}} P \\
 \langle 2,-2 | p^- | 1,-1 \rangle &= P
 \end{aligned}$$

A simple calculation of matrix elements of p^+ , p^- , p_z between (A2) and (A1) yields, using (A3) the following relative oscillator strengths

$$\begin{aligned}
 Q_V(j = \frac{5}{2}) \rightarrow (\frac{3}{2}, \pm\frac{1}{2}) & \quad \frac{10}{3} \\
 Q_{IV}(j = \frac{3}{2}) \rightarrow (\frac{1}{2}, \pm\frac{1}{2}) & \quad \frac{10}{3} \\
 Q_V(j = \frac{5}{2}) \rightarrow (\frac{3}{2}, \pm\frac{3}{2}) & \quad 3 \\
 Q_{IV}(j = \frac{3}{2}) \rightarrow (\frac{3}{2}, \pm\frac{3}{2}) & \quad \frac{1}{3} \\
 Q_{IV}(j = \frac{3}{2}) \rightarrow (\frac{3}{2}, \pm\frac{1}{2}) & \quad \frac{1}{3}
 \end{aligned}$$

We therefore see that the $j = \frac{3}{2} \rightarrow j = \frac{3}{2}$ transitions (corresponding to the minus sign in the linear combinations of equation (A1) and the plus sign in (A2)) are negligible.

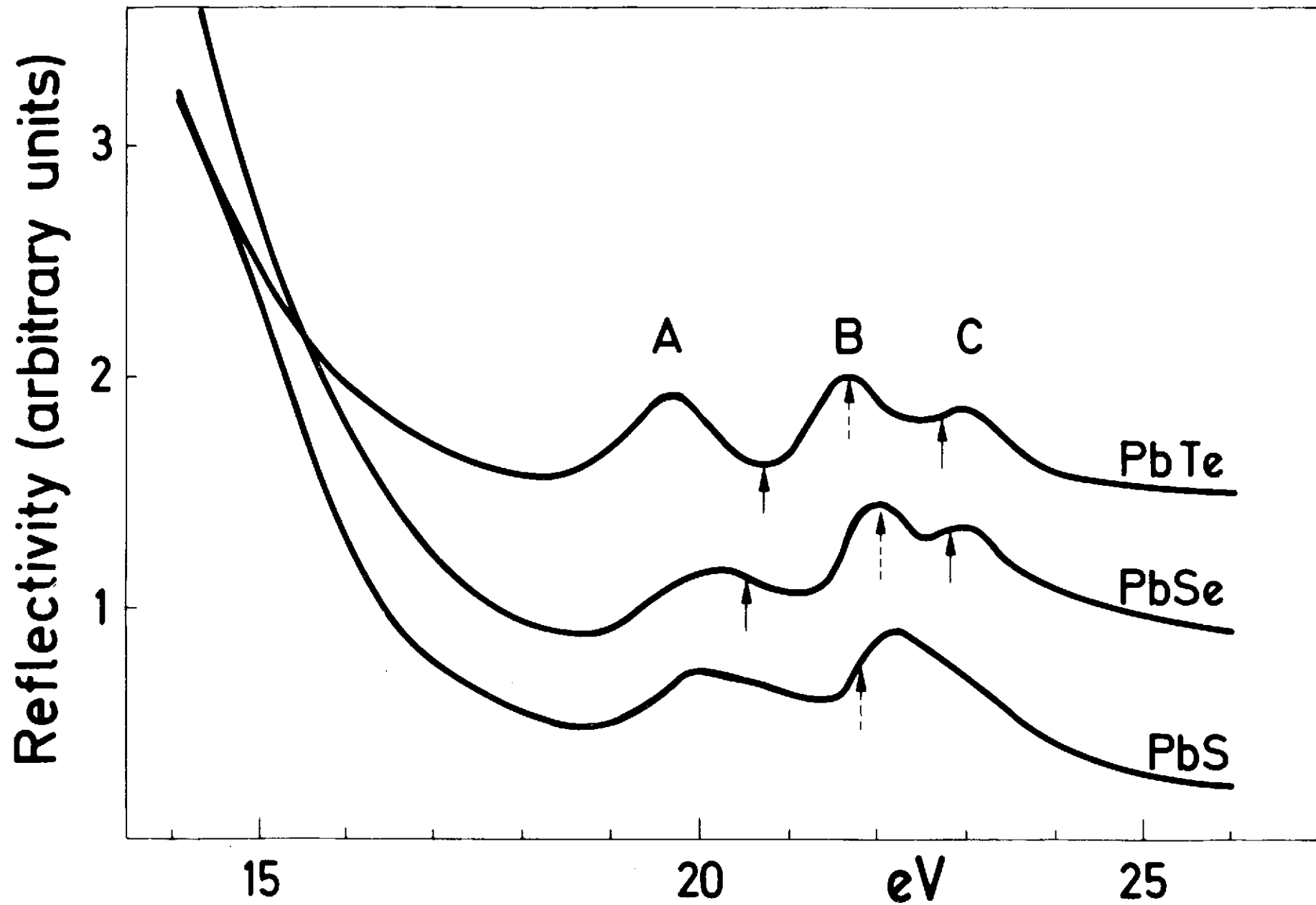


FIG. 1

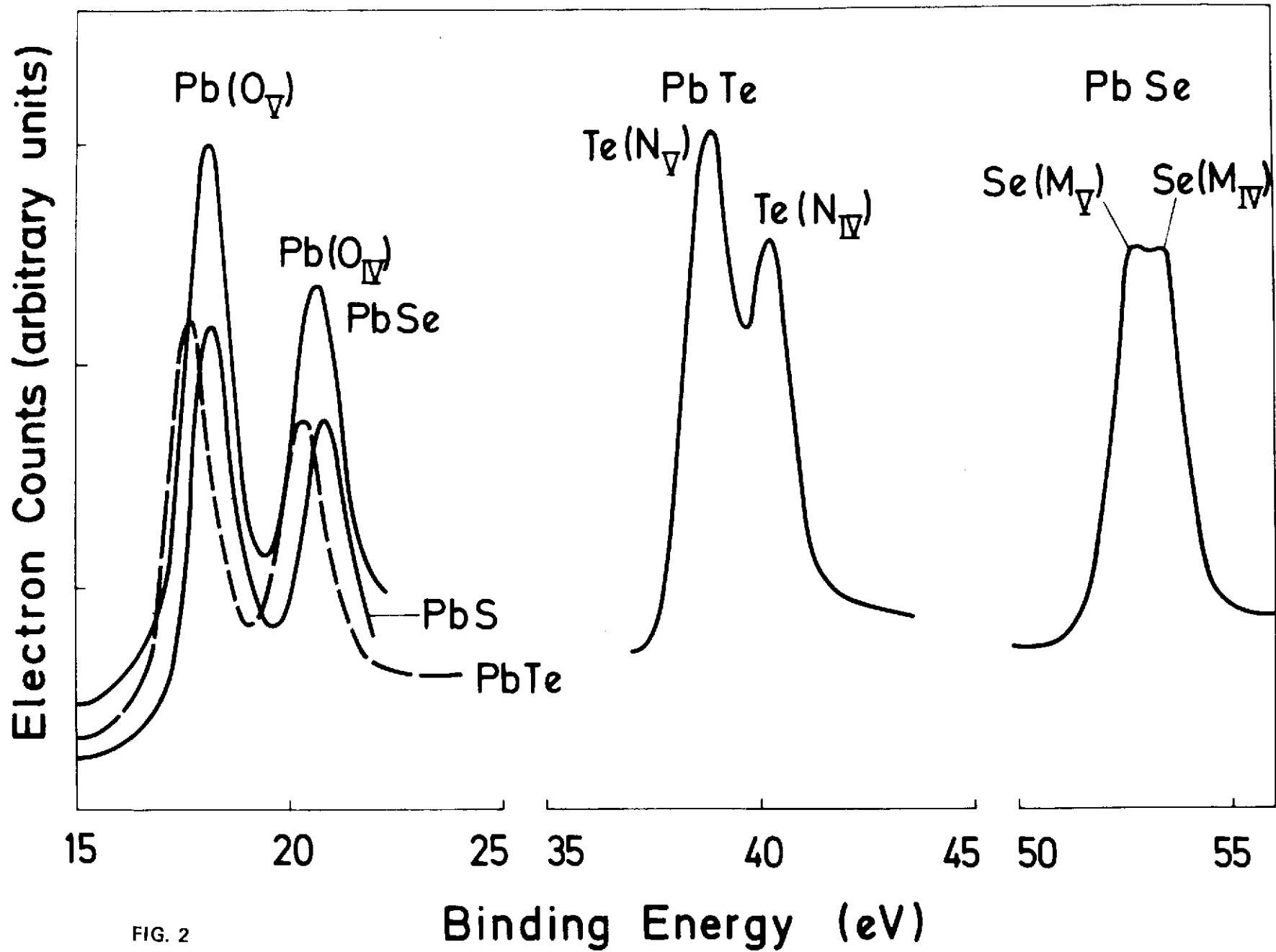


FIG. 2

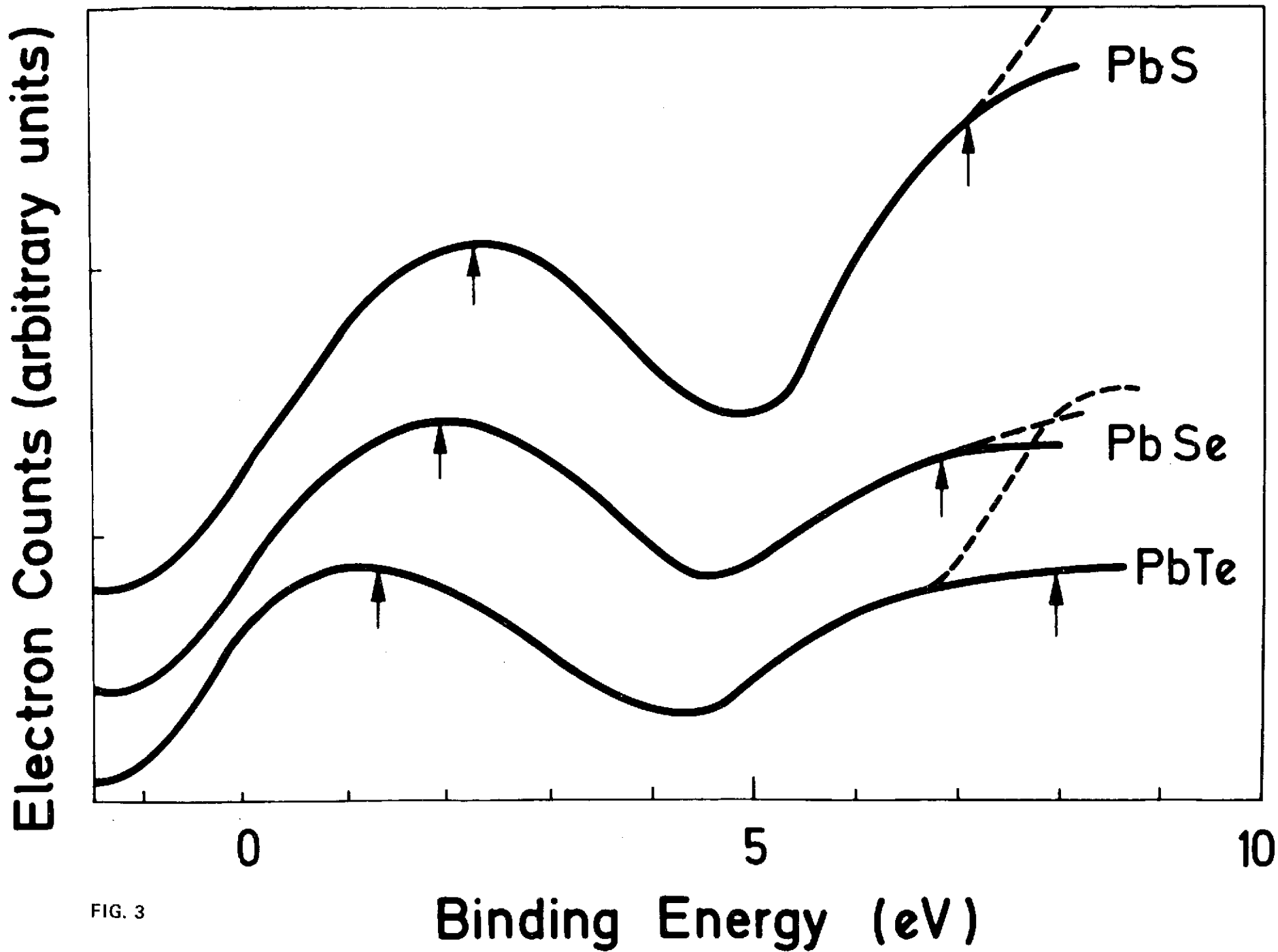


FIG. 3

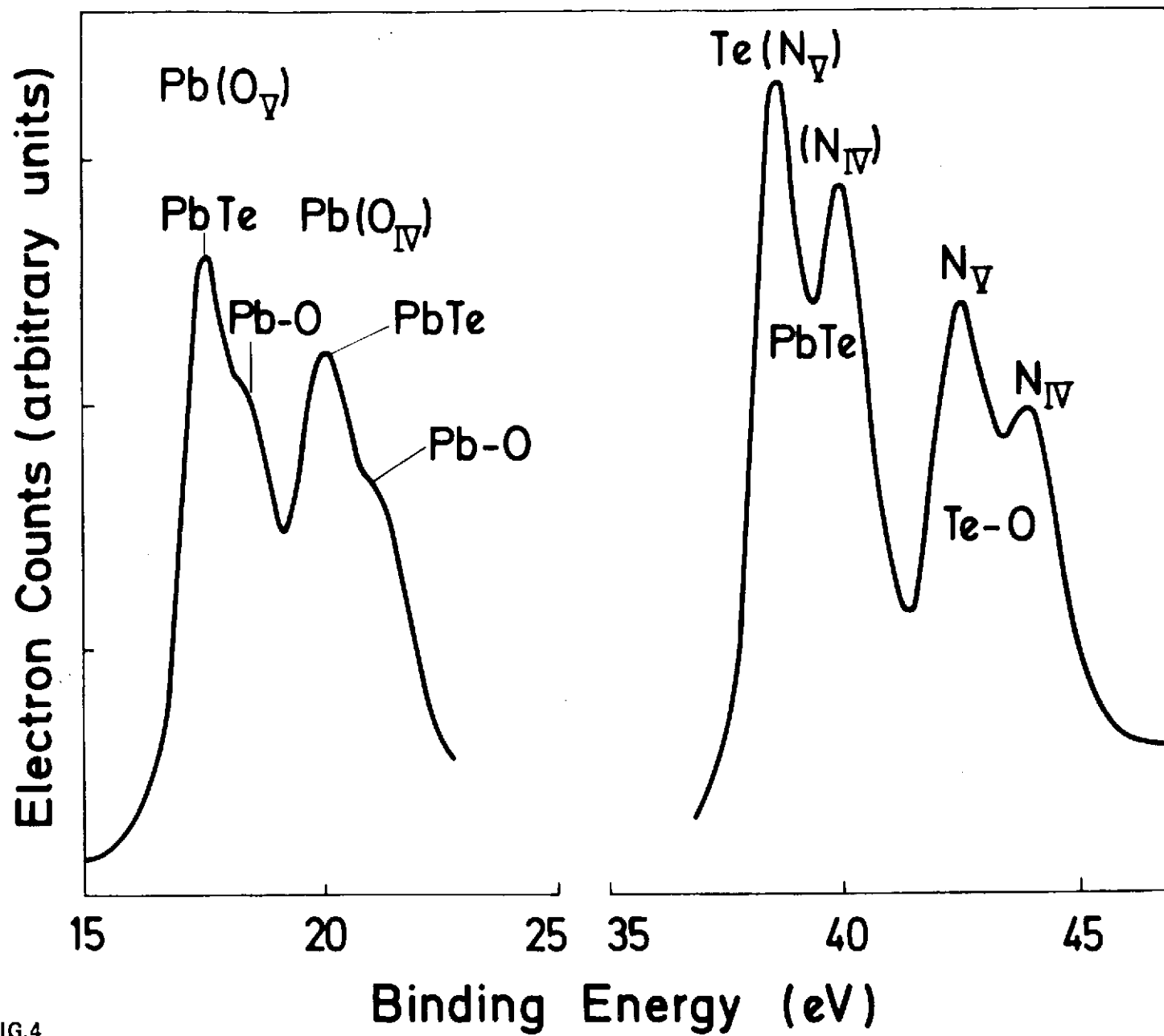


FIG.4

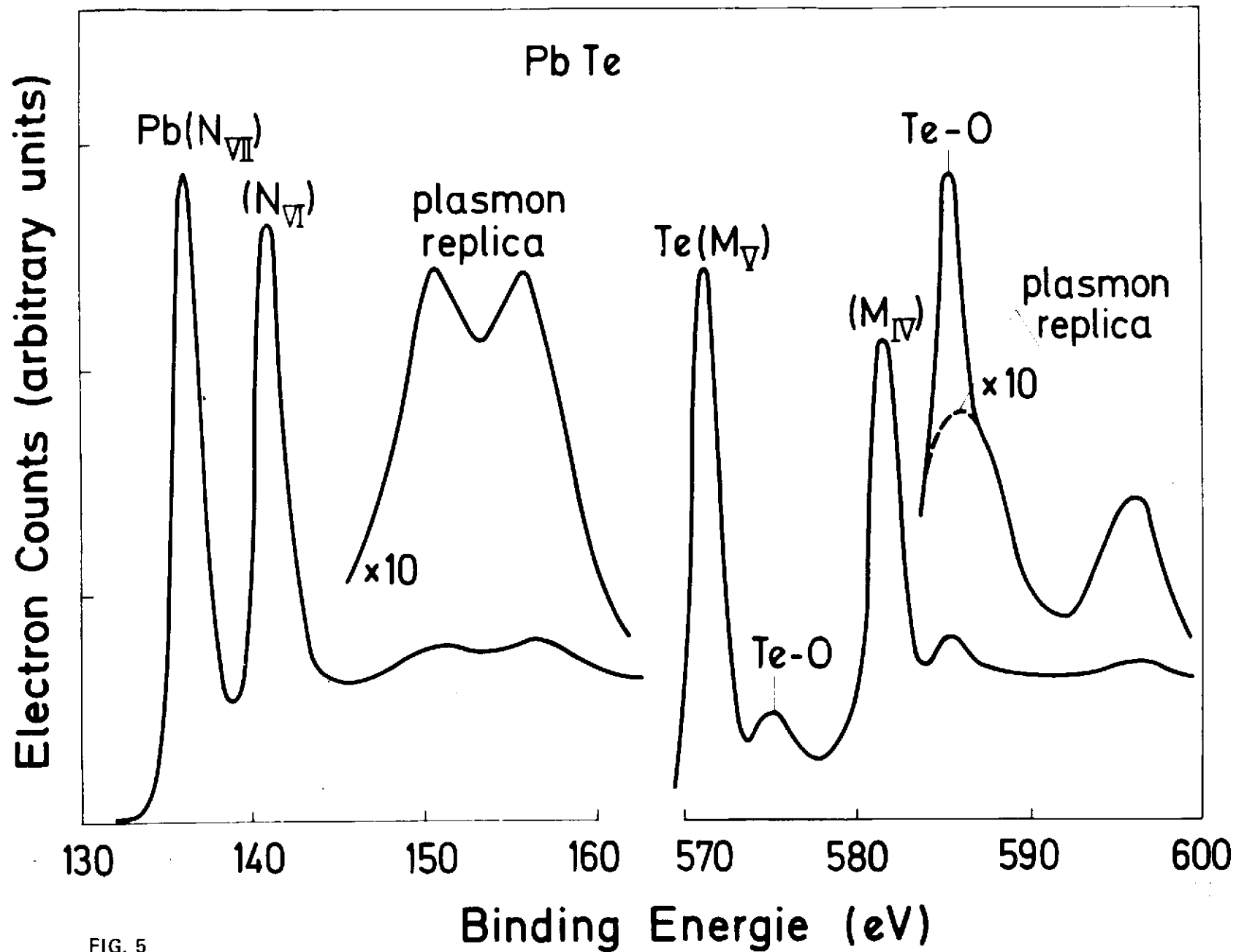


FIG. 5

LEAD TELLURIDE

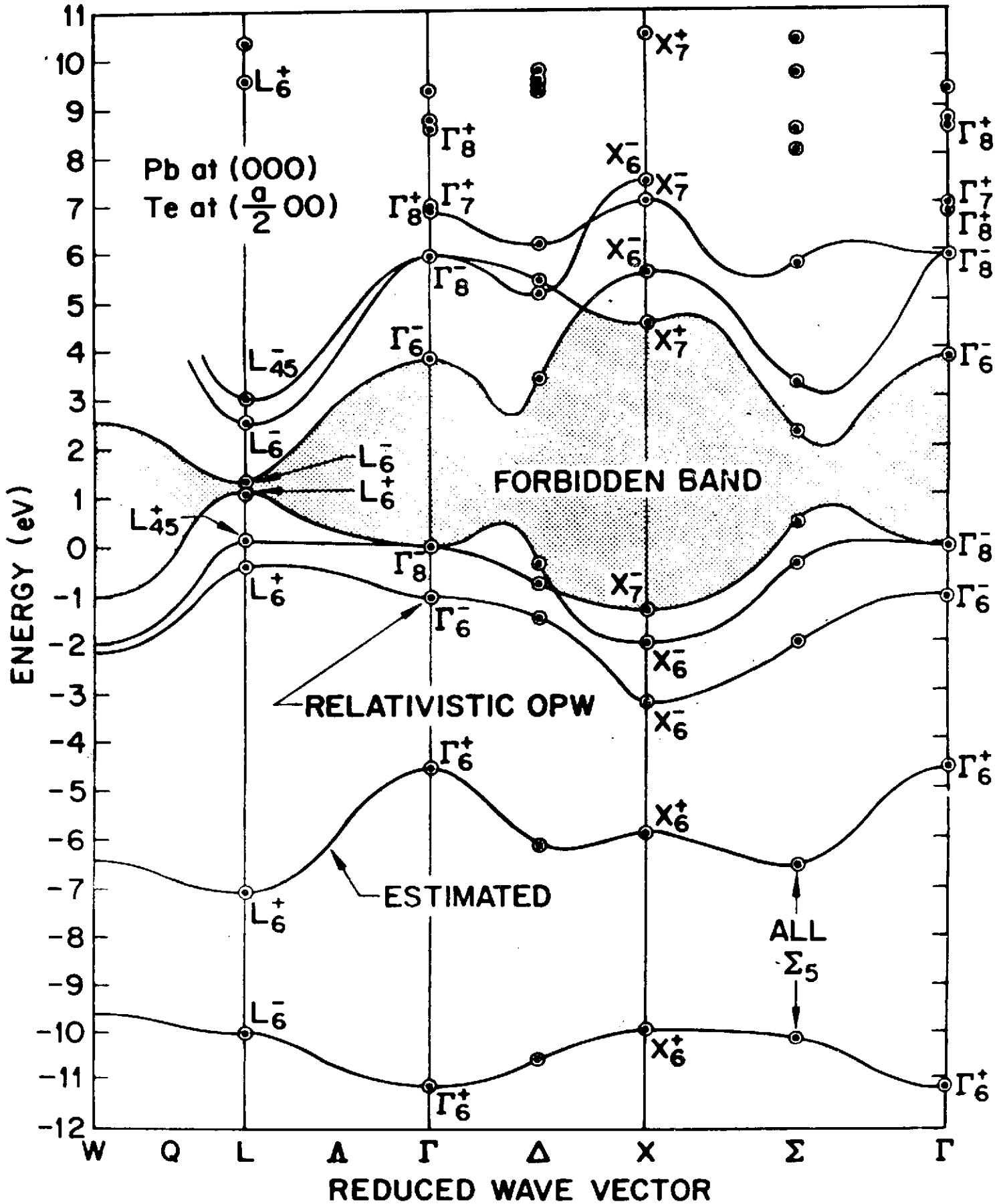


FIG. 6

levels of Pb

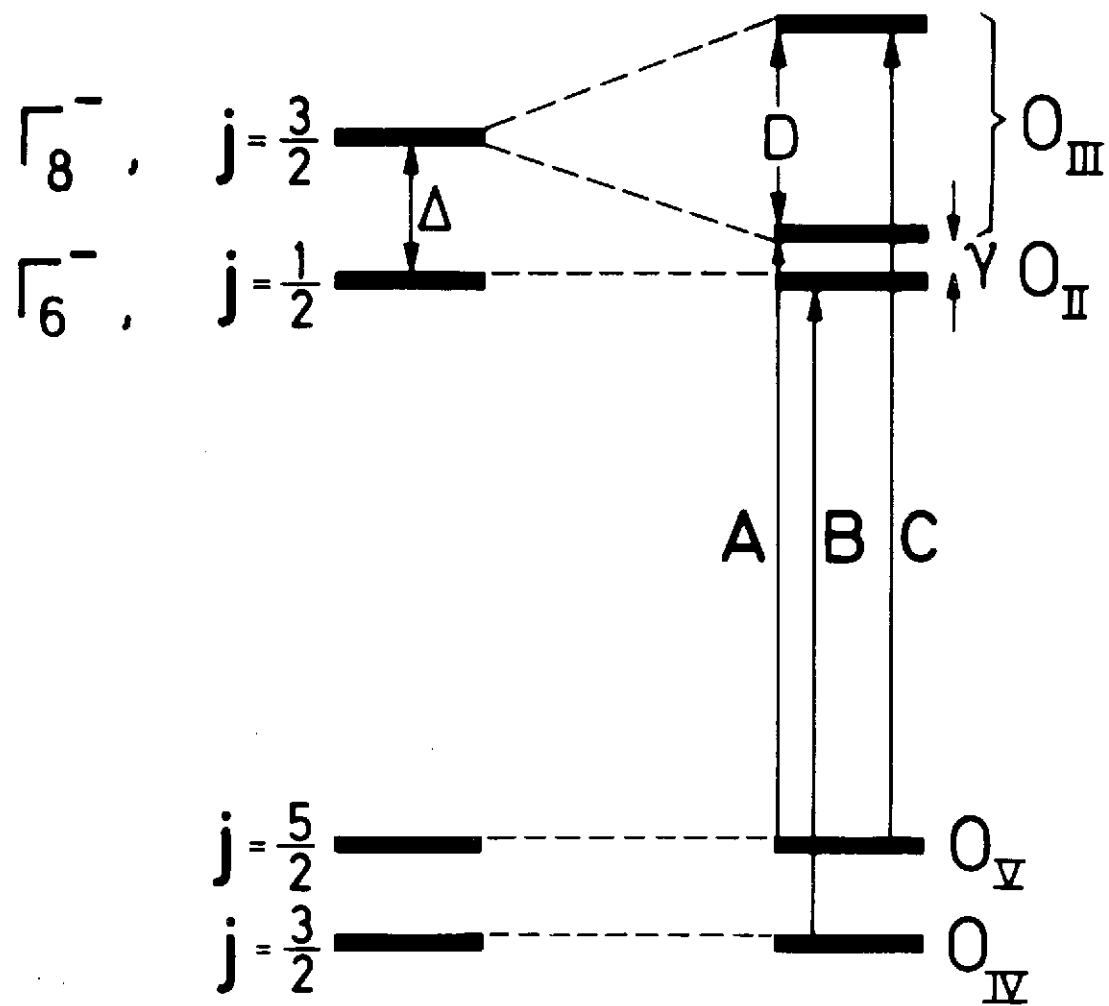


FIG. 7

